Development of a chirped/differential optical fiber Bragg grating pressure sensor

2008 Meas. Sci. Technol. 19 045304

(http://iopscience.iop.org/0957-0233/19/4/045304)

Meas. Sci. Technol. **19** (2008) 045304 (6pp) doi:10.1088/0957-0233/19/4/045304

Development of a chirped/differential optical fiber Bragg grating pressure sensor

Yen-Te Ho, An-Bin Huang and Jui-ting Lee

Department of Civil Engineering, National Chiao-Tung University, Hsinchu, Taiwan

E-mail: yenteho@pchome.com.tw, abhuang@mail.nctu.edu.tw, ruiting.cv92g@nctu.edu.tw

Received 22 June 2007, in final form 7 January 2008
Published 13 February 2008
Online at stacks.iop.org/MST/19/045304

Abstract

With its unique capabilities, the optical fiber Bragg grating has been used as a key component in the development of many sensors. Incorporating the theory of thin plates, the authors have developed an FBG-based pressure sensor by strategically attaching FBGs on the surface of a thin circular plate. The flexural strain in the circular plate induced by pressure applied to the circular plate is sensed by either a single FBG placed radially crossing a neutral point, or two FBGs placed respectively in zones where the strains are of opposite signs. When one FBG is used (i.e., the chirped FBG design), the applied pressure relates to the change in the chirped bandwidth of the FBG reflected waveform. When two FBGs are used (i.e., the differential FBG design), the pressure experienced by the circular plate is correlated to the difference in central wavelength from the two FBGs. In either case the sensing mechanism is immune to temperature fluctuation. The same configuration can potentially be applied for other purposes such as a load cell or displacement transducer. This paper describes the design principles of the FBG pressure sensor and demonstrates its capabilities through laboratory calibrations over a wide range of temperatures.

Keywords: optical fiber Bragg grating, pressure sensor

Introduction

Taking advantage of its unique capabilities, several types of fiber optic sensored pressure transducers have been developed recently (Kashyap 1999, Kojima *et al* 2003, Liu *et al* 2000, Xu *et al* 1993, Yang *et al* 2005, Zhao *et al* 2004). The fiber Bragg grating (FBG) is one of the commonly used means to measure the change of pressure. The currently available FBG-based pressure sensors can generally be divided into two groups according to their modulation schemes. The first group may be referred to as the uniform strain FBG (UFBG) design where the distribution of strain across the FBG remains uniform. In the UFBG design, the change of pressure causes mainly shifting of the central wavelength of the FBG reflected waveform (Heo *et al* 2005, Kashyap 1999, Kojima *et al* 2003, Liu *et al* 2000b, Rao *et al* 1994, Xu *et al* 1996, Zhang *et al* 2001). The second group may be called the chirped fiber Bragg grating (CFBG) design (Dong *et al* 2002), where the change of pressure causes a variation in the bandwidth of the FBG reflected waveform. The variation in bandwidth or chirping of the FBG waveform is a result of non-uniform strain distribution across the FBG. The CFBG design has the advantage over the central wavelength scheme in that the bandwidth of the FBG reflected waveform is practically immune to temperature fluctuation (Xu *et al* 1995). When a CFBG is subjected to a non-uniform strain distribution, there is possibly a change to the reflection profile as well as the bandwidth. The currently available CFBG design however, involves a more complicated mechanical design that may render the transducer less sensitive or limit its use only for the high-pressure range (Zhao *et al* 2004). The authors developed a pressure sensor based on the CFBG scheme. In the new design, referred to as the chirped/differential FBG design or C/D-FBG, a single or a pair of FBGs were attached to the surface of a circular diaphragm. The application of pressure induces a non-uniform strain distribution on the diaphragm. With proper positioning of either a single FBG or two FBGs, the non-uniformity of the strain distribution can be measured according to variations in

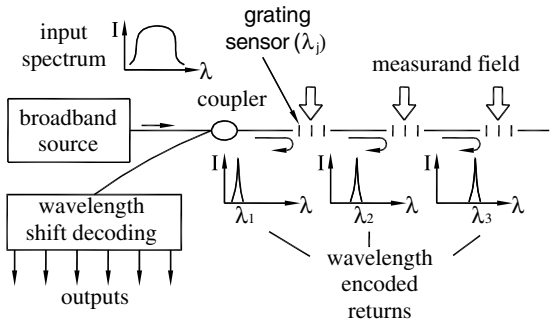

Figure 1. A conceptual description of FBG multiplexing (after Kersey 1992).

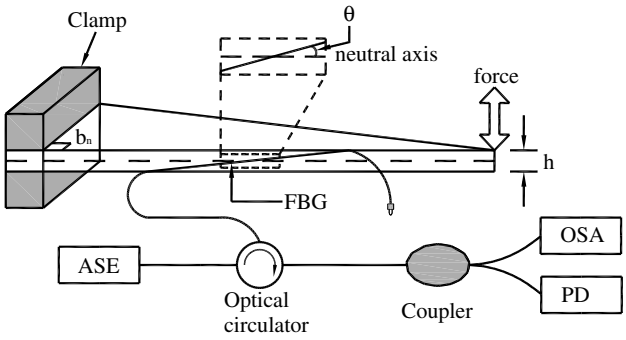

Figure 2. The sketch of a temperature-independent displacement/pressure sensor (after Yang *et al* 2005).

the bandwidth of the reflected waveform from a single FBG or difference of the central wavelengths from the two FBGs. The magnitude of pressure is then determined according to the characteristics of the FBG waveforms. The new design has many important advantages over the currently available FBG-based pressure sensors. The paper provides a brief description of the basic principles of central wavelength and chirped FBG design first and then presents details of the C/D-FBG scheme. In addition to pressure sensing, the advantages of the C/D-FBG and potential applications are also discussed.

The principles of available UFBG and CFBG design

Detailed principles of FBG and its manufacturing can be found in Dyer *et al* (2005), Hill *et al* (1978), Meltz *et al* (1989), Othonos and Kalli (1999) and Rao (1998). The lengths of FBGs are generally within the range of 1 to 20 mm. When the wideband light source illumines an FBG, a fraction of the light is reflected back upon interference by the FBG. When the strain within the FBG is uniform, the reflected waveform has a well-defined peak. This peak wavelength is referred to as the Bragg wavelength λ_B. The longitudinal strain within the Bragg grating, ε_B, induced by variations in temperature or stress causes a change in λ_B or $\Delta\lambda_B$ (in nm or 10^{-9} m). The approximate relationship among λ_B, $\Delta\lambda_B$ and ε_B can be written as follows (Rao 1998):

$$\frac{\Delta\lambda_B}{\lambda_B} = 0.74\varepsilon_B \tag{1}$$

and

$$\Delta\lambda_B = 8.9 \times 10^{-6}\lambda_B\Delta\,^{\circ}\mathrm{C} \tag{2}$$

where $\Delta\,^{\circ}$C is the change of temperature in degree Celsius. The signal returned from an FBG carries a unique domain of wavelength $\lambda_B + \Delta\lambda_B$, making it possible to have multiple FBGs on the same fiber. The multiplexing among various sensors on a single fiber and conceptual description is described in figure 1. The power intensity of the light source becomes weaker when it passes an FBG and a connector, and in normal conditions the maximum number of FBG sensors placed within the same fiber does not exceed 10. A resolution in λ_B of 1 pm to 0.1 pm may be resolved with the currently available FBG integration systems. The UFBG design generally involves a mechanism that causes a uniform straining (ε_B) of the FBG as a result of pressure changes. For an FBG with a given λ_B, the change in pressure is thus modulated through $\Delta\lambda_B$ according to equation (1). A disadvantage in the UFBG design is that $\Delta\lambda_B$ is also affected by fluctuations in temperature as indicated in equation (2). The UFBG design generally incorporates a means to either nullify or account for the temperature effects.

A grating that has a non-uniform and progressively changing period distribution along its length is known as chirped. Detailed principles and structures of CFBG can be found in Kashyap (1999). When the FBG is strained from its original period of Λ_o, the chirped bandwidth relates to the chirped period as (Kashyap 1999)

$$\Delta\lambda_{\mathrm{chirp}} = 2n_{\mathrm{eff}}(\Lambda_{\mathrm{long}} - \Lambda_{\mathrm{short}}) = 2n_{\mathrm{eff}}\Delta\Lambda_{\mathrm{chirp}} \tag{3}$$

where $\Delta\lambda_{\mathrm{chirp}}$ is the change of the chirped bandwidth, n_{eff} is the effective mode index, Λ_{long} is the longest period of CFBG, Λ_{short} is the shortest period of CFBG and $\Delta\Lambda_{\mathrm{chirp}}$ is the period change in the fiber.

According to equation (3) $\Delta\lambda_{\mathrm{chirp}}$ can be made strain dependent if a strain gradient is introduced along the FBG.

Yang *et al* (2005) reported a displacement/pressure sensor based on the CFBG design. An FBG is attached to the side of a triangle cantilever beam at an inclined angle as shown in figure 2 to measure the non-uniform strain distribution. The center of the FBG is located at the neutral axis of the cantilever as shown in figure 2. The sensor is designed so that the applied displacement or pressure causes bending of the triangular beam. An important advantage of this CFBG design is that $\Delta\lambda_{\mathrm{chirp}}$ is practically immune to temperature fluctuation. In order to configure the FBG-sensored beam into a pressure transducer, an additional diaphragm is required to provide the sealing (Yang *et al* 2005). A linkage was used so that the beam and its FBG deform with the diaphragm as a result of pressure application. The sensitivity is thus reduced due to the addition of linkage and separation of the beam and diaphragm.

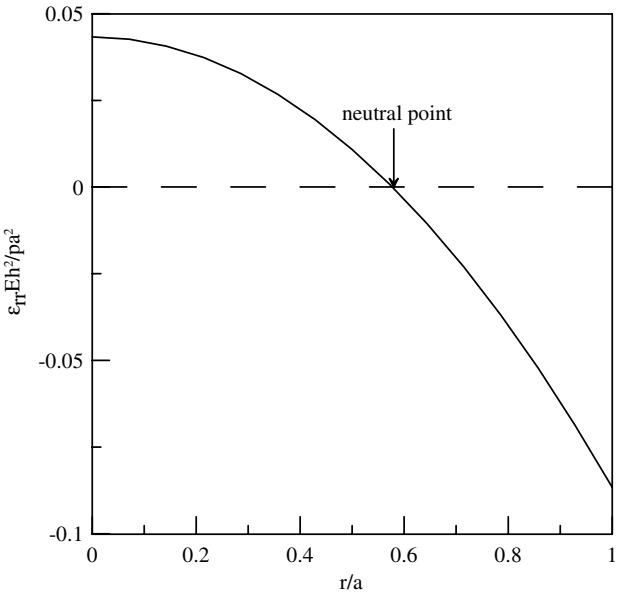

Figure 3. Variation of strain in the radial direction.

Design principles of the C/D-FBG pressure sensor

According to Timoshenko and Woinowsky-Krieger (1959), for a circular thin plate with clamped edges, the amount of deflection (w) perpendicular to the plate surface relates to the uniformly applied pressure (p) and radial distance from the center (r) as,

$$w = \frac{3p(1-\nu^2)}{16Eh^3}(a^2 - r^2)^2 \tag{4}$$

where a is the radius of the plate, E is Young's modulus of the plate material, ν is Poisson's ratio and h is the thickness of the circular plate.

No rotation of the plate (i.e., $\frac{dw}{dr} = 0$) is allowed because of clamping at the edge ($r = a$) and symmetry at the center ($r = 0$) of the plate, thus resulting in a distribution of moment as,

$$M_r = \frac{p}{16}[(1+\nu)a^2 - (3+\nu)r^2] \tag{5}$$

and

$$M_\theta = \frac{p}{16}[(1+\nu)a^2 - (1+3\nu)r^2] \tag{6}$$

where M_r is the moment in the radial direction per unit length and M_θ is the moment in the circumferential direction per unit length.

The maximum bending stress in radial (σ_{rr}) and circumferential ($\sigma_{\theta\theta}$) directions occur on the surface of the circular plate, where

$$\sigma_{rr} = \frac{6M_r}{h^2} \quad \text{and} \quad \sigma_{\theta\theta} = \frac{6M_\theta}{h^2}. \tag{7}$$

According to Hooke's law, strain in the radial direction (ε_{rr}) relates to stresses as,

$$\varepsilon_{rr} = \frac{1}{E}(\sigma_{rr} - \nu\sigma_{\theta\theta}). \tag{8}$$

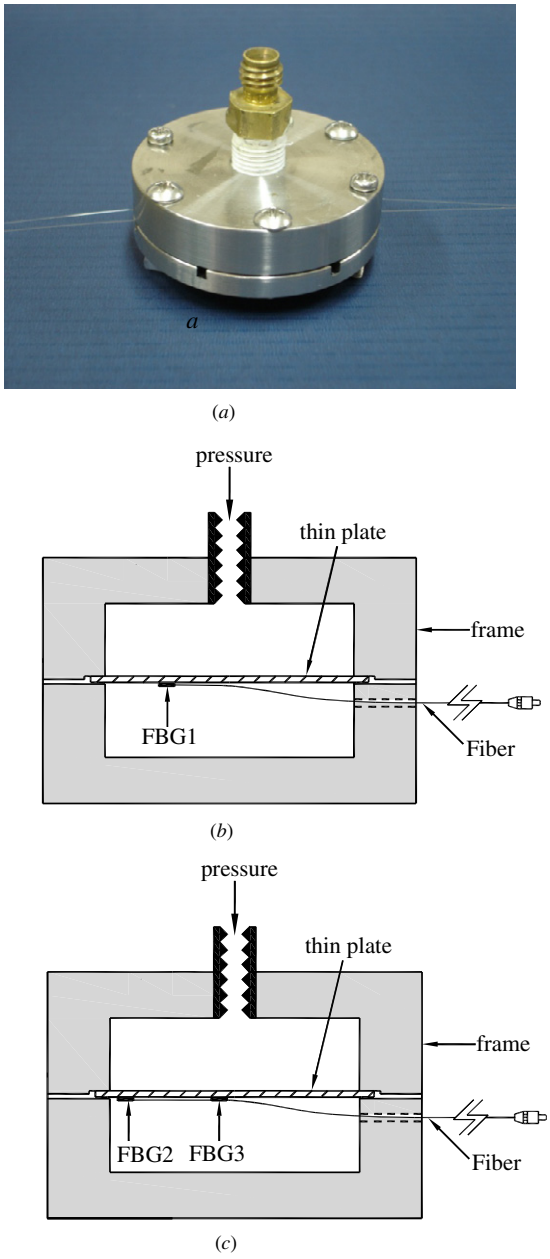

Figure 4. (*a*) Photograph of the pressure sensor. (*b*) Sectional view of the chirped FBG pressure sensor. (*c*) Sectional view of the differential FBG pressure sensor.

(This figure is in colour only in the electronic version)

Combining equations (5)–(8) results in

$$\varepsilon_{rr} = \frac{3p(1-v^2)}{8Eh^2}(a^2 - 3r^2). \tag{9}$$

Figure 3 shows a plot of $\frac{\varepsilon_{rr}Eh^2}{pa^2}$ against $\frac{r}{a}$, assuming that ν equals 0.3. As indicated in figure 3 and equation (9), ε_{rr} becomes zero and changes its sign when $r = a/\sqrt{3}$. The ε_{rr} transforms from compression to tension as r crosses the neutral point at a value of $a/\sqrt{3}$.

If a single FBG is attached to the surface of a circular thin plate in the radial direction, $\Delta\Lambda_{\text{chirp}}$ within the FBG

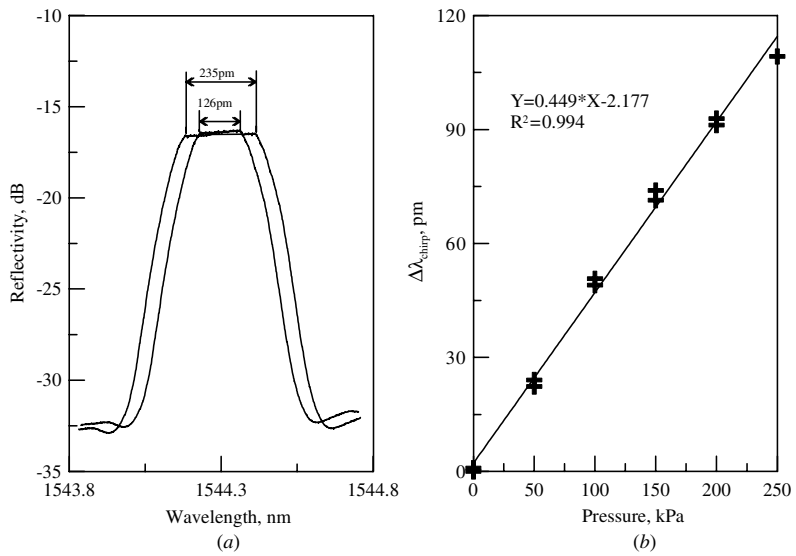

Figure 5. Results of the chirped FBG pressure sensor calibration: (*a*) waveforms at 0 kPa and 250 kPa and (*b*) change of the FBG waveform bandwidth against pressure.

should follow ε_{rr} distribution on the surface of the thin plate. According to the above thin plate theory and equation (3), the FBG should reflect a broadened waveform when the plate is pressurized, because of the non-uniform ε_{rr} distribution. Unless the center of the FBG is aligned at $r = a/\sqrt{3}$, the broadened waveform should also show shifting of the central wavelength.

The new C/D-FBG pressure sensor is constructed by attaching either a single FBG or two FBGs in the radial direction on the surface of a thin circular plate. When a single FBG is used in a chirped FBG design, the center of the FBG is positioned at the neutral point, where $r = a/\sqrt{3}$. According to the above described thin plate theory, the FBG so positioned should generate a broadened waveform with little shifting of its central wavelength when a pressure is applied to the circular plate.

When two FBGs are utilized in a differential FBG design, one of them is attached towards the center of the plate (r is close to 0) and the other close to the clamped edge (r approaches a). The application of pressure should result in central wavelength shifts (i.e., $\Delta\lambda_{B1}$ and $\Delta\lambda_{B2}$) in opposite directions because the two FBGs are located at opposite sides of the neutral point. The applied pressure is modulated by the difference between $\Delta\lambda_{B1}$ and $\Delta\lambda_{B2}$ or $\Delta\lambda_{B1} - \Delta\lambda_{B2}$. Thus, the strength of the signal is enhanced by the subtraction. Due to non-uniformity in strains, the waveforms from both FBGs are also expected to be chirped during pressure application.

The change in temperature induces uniform straining throughout the circular plate. In a chirped FBG design, the temperature fluctuation causes the central wavelength to shift but has no effect on $\Delta\lambda_{chirp}$. In differential FBG design, the temperature fluctuation should cause $\Delta\lambda_{B1}$ and $\Delta\lambda_{B2}$ to change by equal amounts and in the same direction. Thus, $\Delta\lambda_{B1} - \Delta\lambda_{B2}$ should cancel out the effects of temperature fluctuation.

Fabrication and calibration of the C/D-FBG pressure sensor

Following the chirped FBG design, the authors attached a 3 mm long FBG on the face of a 30 mm diameter ($a = 15$ mm) and 0.3 mm thick ($h = 0.3$ mm) 316 stainless steel plate in the radial direction. A steel needle was used to scrape a line on the stainless-steel plate where the FBG was to be attached. A pre-tension of 3000 $\mu\varepsilon$ was applied when bonding the FBG to the surface of the stainless-steel plate using a heat cured epoxy. The center of the FBG was fixed at $r = 15/\sqrt{3}$ or 8.66 mm. Figure 4 shows a photograph and schematic diagram of the pressure sensor. The FBG, attached to the surface of the circular plate, directly senses strains caused by the pressure applied to the opposite side of the plate. The sensor was calibrated in a thermal chamber under 25 °C, by regulated air pressure from 0 to 250 kPa. Results shown in figure 5 indicate a resolution of 2.22 kPa for 1 pm of $\Delta\lambda_{chirp}$, the minimum wavelength shift identifiable by the interrogator. The relatively low sensitivity or change in $\Delta\lambda_{chirp}$ in response to pressure is mainly due to the limited length of the FBG.

The pressure sensor of a differential FBG design had the same physical dimensions as shown in figure 4. The material used for the metal plate and the procedure of attaching the FBG were the same as the chirped FBG design. The major difference is that there were two FBGs attached to the surface of the circular plate, one toward the center and the other close to the edge of the plate. The pressure sensor was calibrated in a thermal chamber under three different temperatures ranging from 25 to 50 °C. The results depicted in figure 6 had a resolution of 0.16 kPa per 1 pm of $\Delta\lambda_{B1} - \Delta\lambda_{B2}$, for the range of 0 to 250 kPa. The resolution in a differential mode is significantly better than that of the chirped FBG design. The results also showed a strong linearity between $\Delta\lambda_{B1} - \Delta\lambda_{B2}$ and pressure, with coefficients of correlations generally higher than 0.99. For a given pressure, $\Delta\lambda_{B1} - \Delta\lambda_{B2}$ deviates no

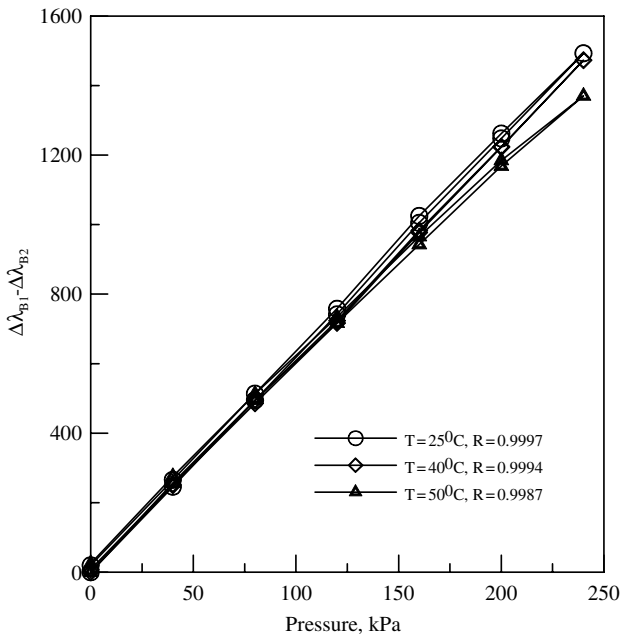

Figure 6. Results of the differential FBG pressure sensor calibrations.

more than 5% from the average value among tests in three different temperatures, indicating that the sensor was largely immune to thermal effects for the range of temperature fluctuation.

According to equations (3), (4) and (9), there should be a linear relationship between $\Delta\lambda_{B1} - \Delta\lambda_{B2}$ and the applied pressure (p) in a differential FBG design. This linear relationship remains if the FBG is properly bonded to the metal thin plate and the pressure induced straining or deformation of the metal plate is not excessive so that E and r remain constant. Results demonstrated in figure 6 showed that for the pressure range applied, there was a reasonable linearity between $\Delta\lambda_{B1}$–$\Delta\lambda_{B2}$ and p. Equation (3) assumes that the grating period within the FBG changed from Λ_{short} to Λ_{long} or vice versa in a linear and monotonic fashion. This implies that ε_{rr} distribution of the thin metal plate where the FBG is attached should be linear in the chirped FBG design. For the pressure sensor described in this paper, the FBG had a length of 3 mm and the radius of the metal plate (a) was 15 mm. The corresponding r/a spanned from 0.477 to 0.677 when the center of the FBG was attached to the neutral point ($r/a = 1/\sqrt{3} = 0.577$) as indicated in figure 3. The distribution of ε_{rr} was close but not exactly linear as shown in figure 3. This may be part of the reason for the less linear performance in the chirped FBG design as described in figure 5.

Conclusions

The authors have developed an FBG-based pressure sensor by strategically attaching either one or two FBGs on the surface of a thin circular plate. When one FBG is used (i.e., the chirped FBG design), the applied pressure relates to the change in the chirped bandwidth of the FBG reflected waveform. When two FBGs are used (i.e., the differential FBG design), the pressure experienced by the circular plate is correlated to the difference in central wavelength variations from the two FBGs. Because of the limited length of FBG used in the design reported herein, the differential design had a better sensitivity to the change of pressure. In either case the sensing mechanism is immune to temperature fluctuation. The FBG signals reflect the difference in pressure between the two sides of the circular plate. Thus, it can be used as a differential or gauge pressure transducer (in reference to the atmospheric pressure).

An important advantage of the design presented herein is that the pressure is applied directly to the circular plate where the FBGs are attached without any intermediate linkage, thus enhancing its sensitivity. Analytical solutions for thin plates with different boundary conditions are readily available. Adopting these solutions, the same design can be modified to sense force as a load cell or a displacement transducer. In the case of a load cell, a concentrated force is applied to the center point of the circular plate. By attaching a displacement rod to a spring to convert displacement to a spring load, the same load cell configuration can be used to modulate displacement.

References

Dong X, Guan B O, Yuan S, Dong X and Tam H Y 2002 Strain gradient chirp of uniform fiber Bragg grating without shift of central Bragg wavelength *Opt. Commun.* **202** 91–5

Dyer S D, Williams P A, Espejo R J, Kofler J D and Etzel S M 2005 Fundamental limits in fiber Bragg grating peak wavelength measurements *Proc. SPIE, 17th Int. Conf. on Optical Fibre Sensors (Bruges, Belgium)* vol 5855 pp 88–93

Heo J S, Chung J H and Lee J J 2005 Tactile sensor arrays using fiber Bragg grating sensors *Sensors Actuators* A **126** 312–27

Hill K O, Fujii F, Johnson D C and Kawasaki B S 1978 Photosensitivity in optical waveguides: application to reflection filter fabrication *Appl. Phys. Lett.* **32** 647–9

Kashyap R 1999 *Fiber Bragg Gratings* (San Diego, CA: Academic Press) p 458

Kersey A D 1992 Multiplexed fiber optic sensors *Proc. Fiber Optic Sensors (Boston, MA)* ed E Udd sponsored by SPIE—The International Society for Optical Engineering, pp 200–27

Kojima S, Hishida Y, Fukuchi K and Hongo A 2003 Optical fiber sensor using fiber Bragg grating for river management *16th Int. Conf. Optical Fiber Sensors (Nara, Japan)* pp 112–5

Liu Y Q, Guo Z Y, Zhang Y, Liu Z G and Dong X Y 2000a Research on the simultaneous measurement of pressure and temperature using one fiber grating *Zhongguo Jiguang/Chin. J. Lasers* **27** 1002–6

Liu Y, Guo Z, Zhang Y, Chiang K S and Dong X 2000b Simultaneous pressure and temperature measurement with polymer-coated fibre Bragg grating *Electron. Lett.* **36** 564–6

Meltz G, Morey W W and Glenn W H 1989 Formation of Bragg grating in optical fibers by a transverse holographic method *Opt. Lett.* **14** 823–5

Othonos A and Kalli K 1999 *Fiber Bragg Gratings: Fundamentals and Applications in Telecommunications and Sensing* (Boston, MA: Artech House)

Rao Y-J 1998 *Fiber Bragg Grating Sensors: Principles and Applications, Optical Fiber Sensor Technology* vol 2 ed K T V Grattan and B T Meggitt (London: Chapman and Hall) pp 355–79

Rao Y J, Jackson D A, Jones R and Shannon C 1994 Development of prototype fiber-optic-based Fizeau pressure sensors with temperature compensation and signal recovery by coherence reading *J. Lightwave Technol.* **12** 1685–95

Timoshenko S P and Woinowsky-Krieger S 1959 *Theory of Plates and Shells* 2nd edn (New York: McGraw-Hill)

Xu M G, Dong L, Reekie L, Tucknott J A and Cruz J L 1995 Temperature-independent strain sensor using a chirped Bragg grating in a tapered optical fiber *Electron. Lett.* **31** 823–5

Xu M G, Geiger H and Dakin J P 1996 Fiber grating pressure sensor with enhanced sensitivity using a glass-bubble housing *Electron. Lett.* **32** 128–9

Xu M G, Reekie L, Chow Y T and Dakin J P 1993 Optical in-fiber grating high pressure sensor *Electron. Lett.* **29** 398–9

Yang X, Dong X, Zhao C L, Ng J H and Peng Q 2005 A temperature-independent displacement sensor based on a fiber Bragg grating *Proc. SPIE, 17th Int. Conf. on Optical Fibre Sensors (Bruges, Belgium)* vol 5855 pp 691–4

Zhang Y, Feng D, Liu Z, Guo Z, Dong X, Chiang K S and Chu B C B 2001 High-sensitivity pressure sensor using a shielded polymer-coated fiber grating *IEEE Photon. Technol. Lett.* **13** 618–9

Zhao Y, Yu C and Liao Y 2004 Differential FBG sensor for temperature-compensated high-pressure (or displacement) measurement *Opt. Laser Technol.* **36** 39–42